IOP Publishing Journal of Physics D: Applied Physics

J. Phys. D: Appl. Phys. **50** (2017) 235301 (9pp) https://doi.org/10.1088/1361-6463/aa6e3e

Pulsed laser deposition of Sr_2FeMoO_6 thin films grown on spark plasma sintered Sr_2MgWO_6 substrates

M Santosh[1], M Lacotte[1], A David[1], Ph Boullay[1], C Grygiel[2], D Pravarthana[1], G S Rohrer[3], P A Salvador[3], P Padhan[4], U Lüders[1], Junling Wang[5] and W Prellier[1]

[1] Laboratoire CRISMAT, CNRS UMR 6508, ENSICAEN, Normandie Université, 6 Bd Maréchal Juin, F-14050 Caen Cedex 4, France
[2] Laboratoire CIMAP, CEA, CNRS UMR 6252, ENSICAEN, Normandie Université, 6 Bd Maréchal Juin, F-14050 Caen Cedex 4, France
[3] Department of Materials Science and Engineering, Carnegie Mellon University, 5000 Forbes Ave., Pittsburgh, PA 15213, United States of America
[4] Department of Physics, Indian Institute of Technology, Madras, India
[5] School of Materials Science and Engineering, Nanyang Technological University, Singapore

E-mail: wilfrid.prellier@ensicaen.fr

Received 15 February 2017, revised 10 April 2017
Accepted for publication 20 April 2017
Published 16 May 2017

Abstract

Sr_2FeMoO_6 (SFMO) films were deposited on polycrystalline spark plasma synthesized Sr_2MgWO_6 (SMWO) substrates. Films were grown using pulsed laser deposition at temperatures (T_{dep}) between 720 °C and 820 °C in a vacuum environment of pressure $P_{dep} = 10^{-6}$ mbar (0.1 mPa); after deposition they were cooled either in a pressure $P_{cool} = P_{dep}$ or $P_{cool} = 10^{-4}$ mbar (10 mPa) O_2. Despite the use of an isostructural substrate, the growth and cooling conditions play the primary role in determining details of the films' structures and properties, similarly to single-crystals. Grazing x-ray and electron back-scatter diffraction indicate that vacuum-cooled films were pure perovskite-structured SFMO exhibiting grain-over-grain growth that aligned the perovskite sub-cells. $SrMoO_4$ impurities were observed in the x-ray patterns for the oxygen-cooled films similarly to single-crystal substrates. Magnetic, electronic and magnetoresistive properties were all a function of growth and cooling environments. The Curie temperature and magnetization of the films increased with T_{dep} up to 800 °C. The vacuum-cooled films had low-resistivities with essentially metallic conductivity (small resistivity increases occurred at low-T), while the conductivity of oxygen-cooled films were consistent with variable range hopping. The oxygen-cooled films had higher low-field magnetoresistance effects at 5 K than the vacuum-cooled films, which seems consistent with $SrMoO_4$ forming at grain boundaries. This work opens the route to tailor the electronic properties by engineering the grain boundaries in thin films.

Keywords: thin films, oxides, pulsed laser deposition

(Some figures may appear in colour only in the online journal)

1. Introduction

Double perovskites (DP) have a parent stoichiometry $A_2BB'O_6$ and a cubic-perovskite based structure in which the B and B' cations order in an alternating fashion along the axes of the primitive cubic-perovskite cell [1, 2]. They are of interest for technological applications because they exhibit various combinations of different functional properties [1–5]. Bi_2NiMnO_6 is ferroelectric and ferromagnetic at low temperatures [6], La_2NiMnO_6 is ferromagnetic and insulating at room temperature [7], and Sr_2MgMoO_6 (SMWO) is a mixed oxide ion/electron conductor at high temperatures [8]. Sr_2TiMoO_6 could also be used for thermoelectric applications [5]. In addition, Sr_2FeMoO_6 (SFMO) is particularly interesting for potential spintronics applications [9, 10] because it is ferromagnetic with a high Curie temperature (410–450 K) and metallic at room temperature, resulting in a half-metallic character (the conduction electrons are fully spin polarized) [9, 10], and exhibits an appreciable low field magnetoresistance (MR) at room temperature [9].

In the ideal SFMO double perovskite structure, the ordered Fe^{3+} and Mo^{5+} ions are located on two interpenetrating equivalent body centered tetragonal sublattices. The magnetic properties of SFMO arise from antiferromagnetic double-exchange interactions between the Fe^{3+} ($S = 5/2$) and Mo^{5+} ($S = 1/2$) ions (sublattices), leading to a theoretical magnetization value of 4 μ_B per formula unit. The fully-ordered structure is also half-metallic, meaning it exhibits nearly full spin-polarization of the conduction electrons [9]. This combination of properties is, however, difficult to realize in thin films appropriate for applications. One of the primary challenges in the synthesis of high quality half-metallic SFMO is to obtain the ideal ordered state with an appropriate stoichiometry. When SFMO is not fully ordered (or when the composition varies from an Fe:Mo ratio of 1:1), Fe and Mo ions sit on the wrong sublattice. When Fe and Mo ions are in Mo and Fe sites, respectively, they are called anti-site disorder. They have been widely observed experimentally and are known to significantly modify the properties [11, 12]. This is believed to occur because the Fe^{3+} (Mo^{5+}) antisite disorder finds itself in an antiparallel configuration with the Fe^{3+} (Mo^{5+}) cations on the regular sites, which reduces the saturation magnetization [13]. Monte-Carlo calculations support this model, indicating the Fe–O–Fe atoms would remain in an antiparallel alignment [14] (though some *ab initio* calculations support a local parallel alignment) [15]. In addition to cationic defects, oxygen vacancies also modify the magnetization of SFMO. In fact, the magnetization reduction of SFMO is four times larger per oxygen vacancy (2 μ_B per vacancy) than per anti-site disorder [16]. Stoeffler *et al* have shown that the half-metallic character is preserved [16], however, for structures containing nearly isolated oxygen vacancies, while it vanishes when anti-site disorder is present, indicating the native magnetic and electronic properties are a complex function of stoichiometry.

In addition to the point defects in the bulk, several extended defects are known to affect SFMO properties. The magnetoresistance of bulk SFMO is thought to arise primarily from the presence of planar defects, such as grain boundaries (GB) (in ceramics and films) or anti-phase boundaries (APBs) (in films). Grain boundaries are disordered regions that result in the insulating barriers to electron transport and exhibit appreciable tunneling magnetoresistance (TMR) at low magnetic fields [17]. In polycrystalline samples of SFMO, the low-field TMR can be readily improved by oxidation of the grain boundaries, which enhances transport across GB barriers [17]. Anti-site boudaries are coherent planar defects across which the cation ordering is perturbed, thereby modifying the local double exchange interactions (akin to anti-site disorder) [18]. Anti-site boundaries occur frequently in films when the nucleation density is high, and the substrate is not selective spatially for the different ordering possibilities. Some authors argue that the low field MR is related to the anti-site boundaries (and anti-site disorder) within the grains, questioning (or ignoring) the role of the GBs [11, 12]. To disentangle whether the GBs or anti-site boundaries primarily dominate the low-field MR, one needs a sample in which the nature and number of all disorders can be controlled.

Most prior work concerning SFMO thin films focused on highly-oriented/epitaxial films grown on a wide range of single crystal substrates [18–24]. Shinde *et al* compared films grown on both polycrystalline and single-crystalline cubic $SrTiO_3$, and demonstrated that the grain boundaries in the film deposited on the polycrystalline substrate exhibited improved low-field MR [21]. Note that the lattice parameters of tetragonal SFMO are $a = 5.57$ Å and $c = 7.90$ Å [25], resulting in a mismatch of SFMO to $SrTiO_3$ of 0.9% (1.1%) along a (c) direction. In this article, we report the magnetic and transport properties of the SFMO grown on polycrystalline SMWO substrates, a well-ordered double perovskite with tetragonal lattice parameters $a = 5.58$ Å and $c = 7.93$ Å [26].

Because SMWO is a non-magnetic and insulating substrate, it will not contribute to the magnetic and conducting properties of SFMO thin films. In addition to better lattice matching, (the mismatch of SFMO with SMWO is 0.2% (0.5%) along the a and c directions respectively, indicating a small tensile strain of the SFMO film), a well-ordered double perovskite substrate may provide an improved driving force for the formation of long-range ordered double perovskite films, and the polycrystalline substrate provides grain boundaries similar to grain boundaries in SFMO ceramics. Since SWMO assists in the spatial selection of the SFMO ordering, avoiding the presence of APBs, these substrates offer the potential of capturing bulk-like properties in thin films of SFMO, especially low-field MR.

Herein we present the pulsed laser deposition (PLD) of epitaxial Sr_2FeMoO_6 films on isostructural polycrystalline Sr_2MgWO_6 substrates, along with characterization of their structural and physical properties. The observations are discussed with respect to both compositional and structural features driven by both growth conditions and substrate structure. A low-field MR associated with substrate grain boundaries is observed and correlated to post-growth annealing procedures. Further optimization of growth on lattice-matched isostructural substrates promises to open the door to new approaches for engineering strain, and extended defects into complex oxides for electronics.

2. Experimental

Thin films of SFMO were grown on polycrystalline SMWO using the PLD technique [27]. The SFMO target and SMWO polycrystalline substrates were prepared by a standard solid state route. The detailed polishing processes of such substrates to obtain mirror-like surfaces appropriate for epitaxial film growth was presented previously [28, 29]. Analysis of the substrates confirm a double-perovskite structure similar to previous reports [30]. The surface morphology is also similar to previous films grown in the same fashion [28]. Thin films of Sr_2FeMoO_6 (200 nm thick, measured via XRD on single-crystals) were deposited onto Sr_2MgWO_6 polycrystalline substrates using PLD with a KrF laser (1.6–1.8 J cm^{-2}, 3 Hz). The growth rate was approximately 0.1 Å per pulse. The base pressure of the chamber was 10^{-6} mbar (0.1 mPa). After deposition, films were cooled down to room temperature at a rate of 20 °C min^{-1} in a pressure of $P_{cool} = P_{dep}$ (vacuum cooled) or $P_{cool} = 10^{-4}$ mbar (10 mPa) of O_2 (oxygen-cooled). Such low pressure is similar to previous reports [26]. The growth was optimized by varying the deposition pressure (P_{dep}) and the deposition temperatures (T_{dep}, ranging from 720 °C to 820 °C), corresponding to the maximum in average image quality (IQ) in electron backScatter diffraction (EBSD) patterns, as described previously [28].

The crystal structure of the SFMO was studied using grazing x-ray diffraction (GXRD) with an incident angle ranging from 0.3° to 1°, to reduce the substrate contribution to x-ray patterns. A Bruker D8 Discover diffractometer was used in θ–θ geometry with a Gobel mirror, providing a parallel x-ray beam for better control of the incident angle. To demonstrate grain-over-grain local epitaxial growth, films were characterized with EBSD, on a scanning electron microscope (20 KV with a working distance of 15 mm). Backscatter Kikuchi patterns were recorded and indexed automatically using EDAX orientation imaging microscopy (OIM^{TM}) software (v. 6.2) [28].

The magnetization-temperature dependence (M-T) of various thin films was measured using a SQUID magnetometer (superconducting quantum interference device, Quantum Design^{TM}), after cooling the sample from room temperature down to 5 K in the presence of a magnetic field (H) of 0.1 T, applied perpendicular to the surface of the film. The field-dependence of magnetization (M-H) was recorded at 15 K, after cooling the film from room temperature in the absence of magnetic field (H). The background of the substrate was measured in similar conditions (field, temperature), and subtracted from the data. Curie temperature (T_C) was calculated from the slot of the (M-T) curves. The resistance (R) of these samples were measured at various temperatures (T), with and without a magnetic field, in a four probe geometry using a Physical Property Measurement System (PPMS, Quantum Design, USA). Magnetoresistance (MR) is defined as $MR(\%) = 100 \times (R(H) - R(0))/R(0)$ where R(H) and R(0) are the resistance values at magnetic field of H and 0, respectively.

3. Results and discussion

Figure 1 shows the GXRD patterns of five thin films prepared under various conditions. All GXRD patterns shown in the figure were recorded at a grazing incidence angle of 0.3°, for which the contribution of the substrate to the GXRD patterns is negligible [28]. Indeed, in separate GXRD experiments (not shown) where the incident angle was varied, an increase of the incident x-ray angle led to a shift in the peaks associated with the substrate phases towards smaller two-theta angles (larger *d*-spacings). For example, the maximum intensity peak for the film deposited at 800 °C has a *d*-spacing of 2.793 Å (film dominated) for a low incident angle of 0.3°, and the *d*-spacing is equal to 2.800 Å (substrate dominated) at an incident angle of 1°. This indicates that the film adopted a structure similar to the substrate.

GXRD analysis of patterns from films deposited at 720 °C exhibited lower intensities than the films deposited at higher T_{dep} of 780, 800, and 820 °C. The average image quality (IQ) in EBSD patterns behaved similarly: the IQ from the film deposited at 720 °C was significantly lower than from the films at higher T_{dep} (the IQ was highest for the film grown at 800 °C). These growth temperature dependent diffraction effects are attributed to improved crystallinity for the films grown in higher temperatures, owing to improved kinetics during growth (the reduction in the IQ for the film with $T_{dep} = 820$ °C suggests that $T_{dep} = 800$ °C optimizes crystallinity).

We observed, for the film grown at 720 °C and oxygen cooled, a peak at 27.7° (highlighted as an inset of figure 1), which corresponds to a $SrMoO_4$ impurity, whereas vacuum cooled films exhibit only peaks from the SFMO phase. $SrMoO_4$ impurities are often observed in SFMO thin films deposited in high oxygen environments [25]. But our films were grown in reducing environments and the $SrMoO_4$ should form only after annealing in oxygen. It has been reported that $SrMoO_4$ impurities exist at grain boundaries in ceramics annealed in oxidizing environments [17, 31]. Since our films are grown on polycrystalline substrates, the $SrMoO_4$ phase could exist at the grain boundaries inherited from the substrate, similar to ceramics. Shinde *et al* also suggested that the grain boundaries inherited from the polycrystalline $SrTiO_3$ substrate were similar to ceramics when oxidized [21].

We estimated the $SrMoO_4$ content to be around 7% (based on the intensities of the SFMO and $SrMoO_4$). The existence of the Mo-rich phase indicates that Fe- and Mo-rich regions exist within the SFMO film. In the present case, the GXRD of all SFMO thin films does not exhibit any signature of Fe-rich phases, whether cooled in vacuum or in oxygen. It has been reported that the SFMO films grown at higher temperatures in oxygen deficient atmospheres favor the formation of oxygen non stoichiometric SFMO ($Sr_2FeMoO_{6-\delta}$) [32], as well as Fe-rich phases, such as $Sr_2Fe_{1+x}Mo_{1-x}O_{6-\delta}$, Fe_3O_4, or metallic Fe [33]. The absence of Fe-rich impurity phases indicates that the grains are likely to have Fe-rich regions of $Sr_2Fe_{1+x}Mo_{1-x}O_{6-\delta}$. The $SrMoO_4$ phases is consistent with $Sr_2Fe_{1+x}Mo_{1-x}O_{6-\delta}$ grains with Mo-rich grain boundaries,

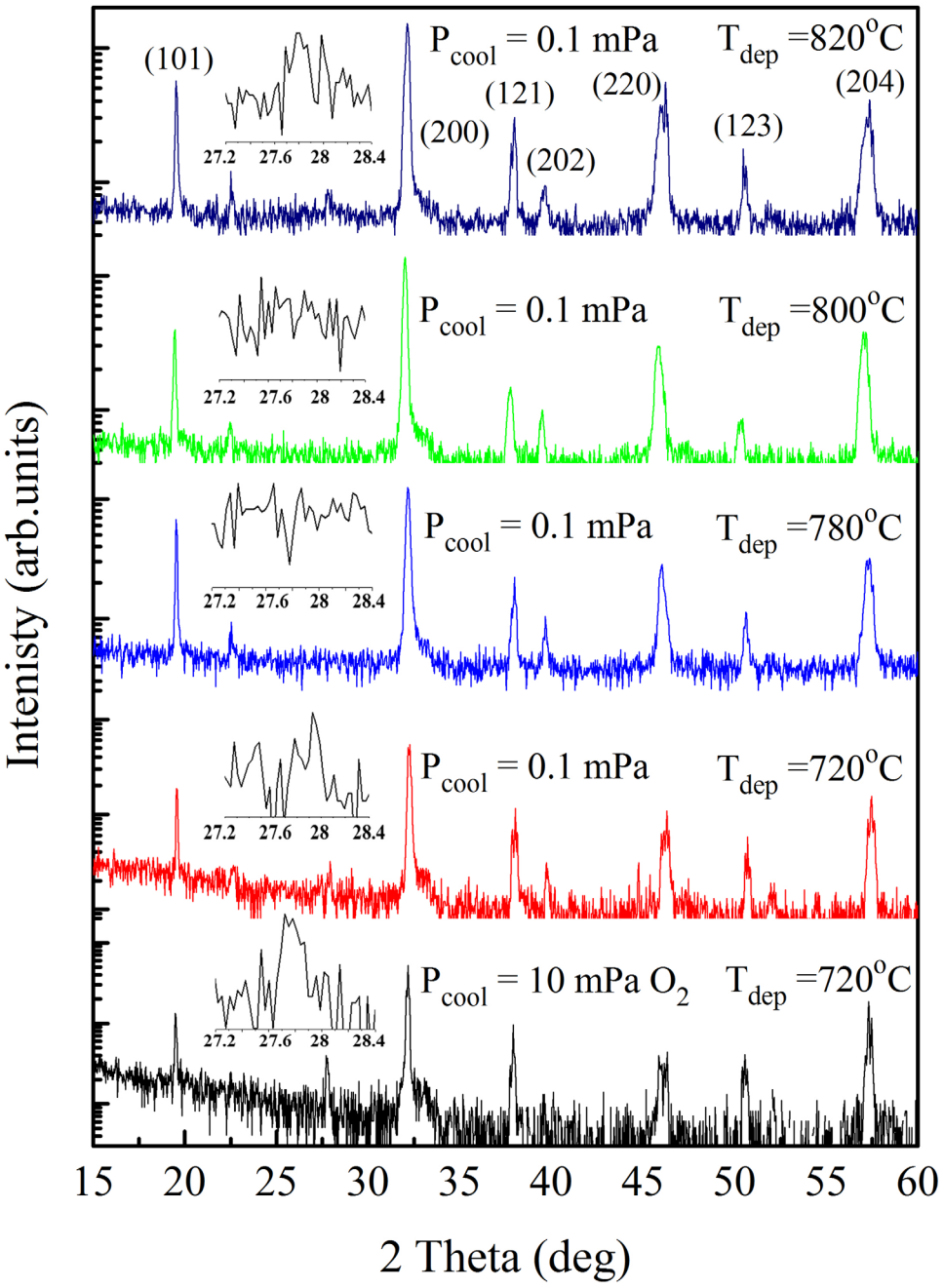

Figure 1. Grazing x-ray diffraction patterns of 200 nm SFMO thin films deposited on polycrystallines SMWO, and grown at various temperatures (T_{dep}) and different cooling conditions. The grazing angle is 0.3°. Insert shows a zoom in the 27–28° region.

similar to earlier reports [19], though the spatial distribution of Fe- and Mo-rich regions was not directly investigated. It is possible that the decreased IQ in EBSD patterns for $T_{dep} = 820$ °C arises from increased vacancy concentration or cation segregation at the higher temperatures, degrading the structural quality and making 800 °C the optimal deposition temperature.

To determine if local epitaxy prevails, EBSD was carried out. Epitaxy would allow the grain boundaries from the substrate to propagate into the film, similar to the epitaxial films grown on rolling assisted biaxially textured substrates [34]. It is important to keep in mind that the tetragonal double perovskite (DP) structure is derived from an underlying pseudo-cubic sub-cell. The three distinct $\langle 1\,0\,0\rangle_c$ cubic perovskite axes transform to two $\langle 1\,1\,0\rangle_{tetragonal}$ and one $\langle 0\,0\,1\rangle_{tetragonal}$ directions in the tetragonal structure. The standard EBSD analysis software does not easily distinguish between the distinct DP orientations, yielding two or three orientations per individual grain that are essentially the same with respect to the pseudocubic perovskite sub-cell. This is shown in figure 2(a), which is the raw inverse pole figure (IPF) map from the SMWO substrate. Nearly all pixels are well-indexed to the tetragonal double-perovskite structure. While clear color regions reminiscent of grains are observed, such regions have two or three distinct colors (corresponding to the equivalent pseudocubic orientations of the tetragonal cell). In other words, even though the

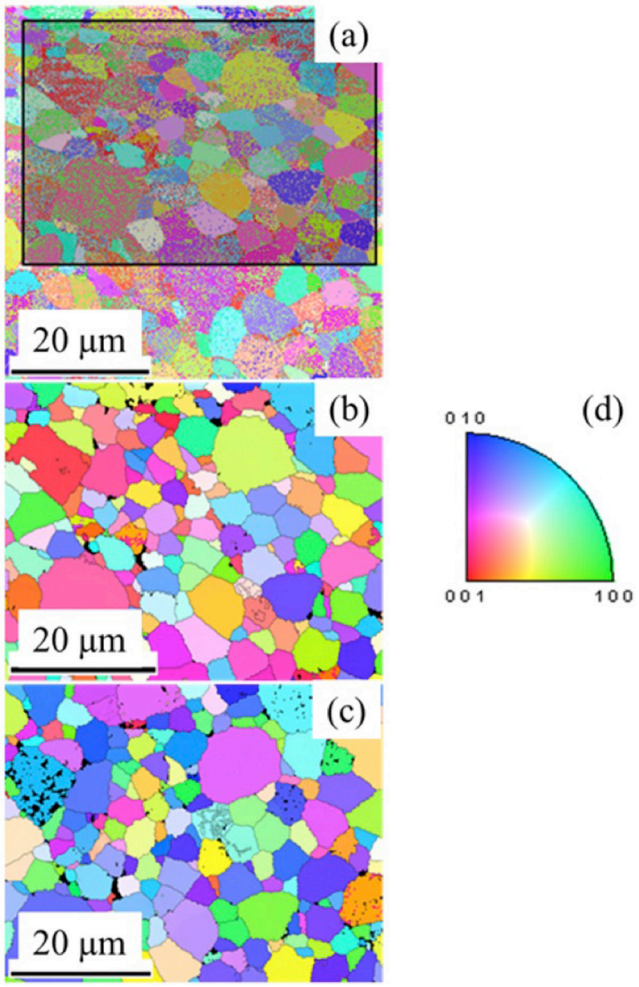

Figure 2. (a) Raw and (b) processed IPF maps from a similar region (marked in (a) by a grey rectangle) of the SMWO substrate. (c) Processed IPF map of the SFMO film from the region to the substrate. 55 pairs of substrate-film grains were analyzed in (b) and (c). Shaded region in (a) indicates the region of our interest.

substrate is a perfectly ordered double perovskite, standard EBSD indexing and mapping does not confidently distinguish the local order as reflected in the precise DP orientation. During the clean up procedures, the orientation of a given grain is assigned to only one of the similar DP orientations (usually the majority). The processed IPF map of the SMWO substrate is shown in figure 2(b).

A similar story occurs for the films. The raw IPF from the vacuum-cooled film (not shown) deposited at $T_{dep} = 800$ °C is similar to figure 2(a). The processed IPF map from that SFMO film is shown in figure 2(c). The shapes of the grains between the films and substrates are very similar, and 55 film-substrate grain pairs are marked in figures 2(b) and (c). Though the shapes of grains are similar, the colors do not always match directly. On analyzing the epitaxial relationships of these 55 grains, 51 of the 55 (93%) align the perovskite sub-cells (the $\langle 1\,1\,0\rangle_{tetragonal}$, $\langle 1\bar{1}0\rangle_{tetragonal}$, and $\langle 0\,0\,1\rangle_{tetragonal}$ are being aligned with each other in degenerate fashions). This indicates that strong local-epitaxy occurs and that local orientation will vary strongly near the original grain boundaries in the substrate [35]. It also confirms that the film grows in a grain-over-grain fashion [29]. On the other hand, to determine if the local DP structure of the substrate influences local tetragonal order in the film requires more careful analysis of the EBSD patterns (which is outside the scope of this work). We did not search for spatial distribution in second phases because the tetragonal phase indexed well throughout the grains (using the current step size) and isolating features along grain boundaries is beyond the scope of this work.

The temperature-dependent magnetizations of the vacuum-cooled and oxygen-cooled SFMO thin films grown at 720 °C are shown in the figure 3(a). The magnetization of the vacuum-cooled (oxygen-cooled) SFMO thin film increases very slightly on cooling from 400 K to 295 K (263 K). The non-zero value in this region may indicate Fe-rich regions (i.e. nonstoichiometric Fe: Mo ratio) with higher ordering temperatures, though the signal is quite low [36, 37]. The magnetization increases rapidly below the onset temperature of 295 K (263 K), which is followed by a more gradual increase down to the lowest temperature. All films exhibited qualitatively similar magnetization curves, and we assigned the Curie temperature (T_C) to the onset temperature of the rapid increase in magnetization. The variation of the Curie temperature T_C with T_{dep} and P_{cool} is shown in the figure 3(b). As T_{dep} increases from 720 °C to 800 °C, T_C increases from 295 K to 320 K. However, on further increase in T_{dep} to 820 °C, T_C is reduced. This observation of an optimal T_{dep} for T_C is similar to the optimal T_{dep} for the IQ in EBSD, suggesting a strong correlation between the crystallinity and magnetization [28]. The T_C for oxygen-cooled films is reduced from that of the vacuum-cooled films for all deposition temperatures (as is the overall magnetization), indicating that oxygen cooling affects the bulk magnetization, decreasing the cooperative ordering temperature and the overall magnetization.

It should be noted that the observed T_C of all SFMO thin films grown on polycrystalline SMWO is lower than that of bulk SFMO, which is 410–450 K [9]. Decreased T_C values in the literature are usually correlated with anti-site disorder, influenced by the non-stoichiometry in the Fe:Mo ratio (Fe-rich leads to the $Sr_2Fe_{1+x}Mo_{1-x}O_{6-\delta}$ composition). This is also evident from the broadening in magnetic transition, as observed in figure 3(a). Anti-site disorder will affect the Fe/Mo ordering, leaving antiferromagnetic $SrFeO_3$ regions that reduce the magnetization and Curie temperature [12, 36, 38]. An excess of Fe has also been reported to segregate to grain boundaries, forming metallic conduction paths across the grains [36]. The lower value of T_C could also be due to the presence of strain and magnetic disorder at the grain boundaries, deviation of Fe and Mo ions from the stoichiometry ratio and the anti-site disorder. However, figure 3(b) indicates that the films cooled with the as deposited pressure has higher T_C compared to that of the films cooled in oxygen ambient, which was attributed to the oxygen vacancy [10].

Figure 4(a) shows the field-dependence magnetization (M(H)) of the vacuum-cooled and oxygen-cooled polycrystalline SFMO films grown at 720 °C. These thin films show a hysteresis in the field dependent magnetization, but do not show clear saturation behaviors at 1 T. The magnetization of the vacuum-cooled SFMO thin film is higher than that of

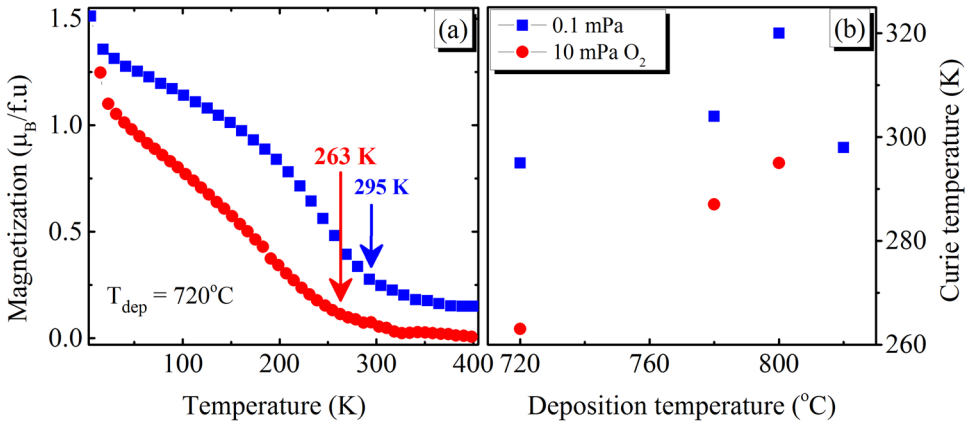

Figure 3. (a) Magnetization as a function of temperature of SFMO films grown at 720 °C on polycrystalline SMWO under different pressures (measurements were made in 0.1 and 0.5 T, respectively for the vacuum-cooled and oxygen-cooled films). Curie temperature, calculated from the slope of the curve is indicated by an arrow (see text for details). (b) Curie temperatures of a series of SFMO films grown on SMWO polycrystalline substrates, plotted as a function of the deposited temperature. In both plots, films cooled in oxygen (vacuum) are given by red circles (blue squares).

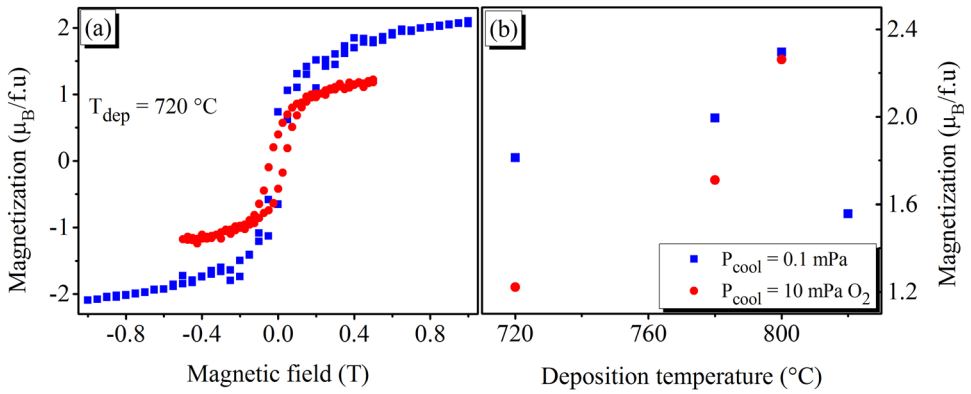

Figure 4. (a) Field-dependence magnetization of SFMO films grown at 720 °C on polycrystalline SMWO at 720 °C. Contribution of the SMWO substrate was subtracted. (b) Magnetization (measured at 0.5 T) versus deposited temperature (T_{dep}) of various SFMO films on polycrystalline SMWO substrates. In both plots, films cooled in oxygen (vacuum) are given by red circles (blue squares).

the oxygen-cooled SFMO film. The magnetization measured at 0.5 T was extracted from the M(H) curves for all SFMO films and is plotted as a function of T_{dep} in figure 4(b). The magnetization of the SFMO thin films increases as T_{dep} increases from 720 °C to 800 °C, but decreases significantly when $T_{dep} = 820$ °C. Additionally, as T_{dep} increases, the difference between the magnetization of the vacuum-cooled and oxygen-cooled samples decreases (they are more similar). At $T_{dep} = 800$°C the magnetization is essentially the same for both cooling conditions. This implies that at the optimal deposition temperature, the structural improvements also render the films more resistant to oxidation effects in the bulk. At the optimal T_{dep}, the magnetization is approximately 2.6 μ_B per formula unit (f.u.). This is considerably lower than the ideal value of 4 μ_B f.u.$^{-1}$. However, the magnetic moment of SFMO at low-temperature is often found to be about 3–3.5 μ_B [13, 20, 39, 40]. Oxygen vacancies, anti-site disorder, and non-stoichiometry in the Fe:Mo ratio can affect the magnetization. Since the magnetization of the oxygen-cooled SFMO films are lower than those of the vacuum-cooled SFMO films, a reduction of magnetization due to oxygen deficiency can be ruled out. The role of anti-site disorder has been studied for thin films [41], for which the suppression rate of magnetic saturation with anti-site disorder is lower compared to polycrystalline SFMO [13], contradicting the Monte-Carlo simulation studies [14]. Nevertheless, this suggests that the use of ceramic helps to improve the parameters, only at given growth conditions when compared to single-crystal growth.

Balcells *et al* observed a decrease of the saturation magnetization proportional to the antisite concentration [13]. They observed magnetization is reduced by 8 μ_B per antisite (0.08 μ_B per 1% of antisite concentration), which is in agreement with a simple ionic model. We estimated the magnetic saturation (at larger magnetic fields) for the film deposited at 800 °C to be ≈2.6 μ_B f.u.$^{-1}$. Assuming anti-site disorder causes the reduction in magnetization, we estimate the ordering parameter is ≈82% [18]. This value is considered as an ensemble average, as the local order parameter could vary with the orientation of the substrate grain, depending on local driving forces and growth kinetics. The significant reduction of magnetization compared to ideal 4 μ_B f.u.$^{-1}$ can be due to the non-stoichiometry induced antiferromagnetic $SrFeO_3$ regions that compete with the parent ferrimagnetic SFMO. Overall, these effects act to decrease magnetization, and to induce magnetic

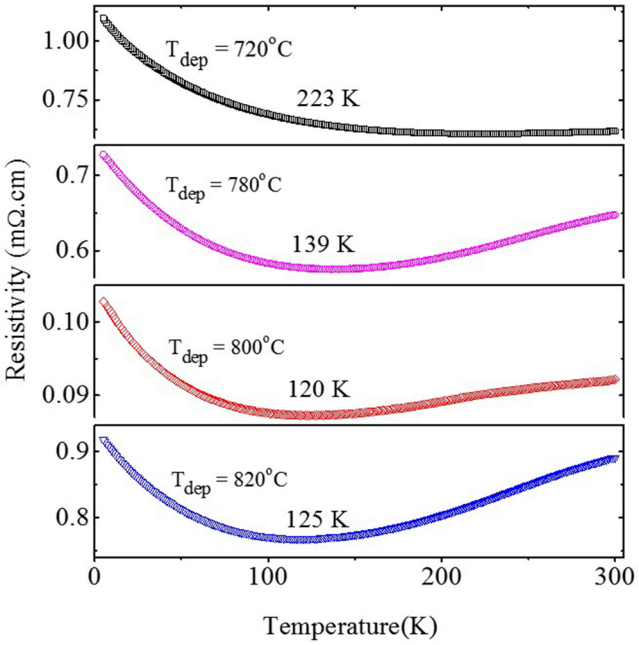

Figure 5. Temperature dependent resistivity of several vacuum-cooled SFMO films grown on polycrystalline SMWO at deposited temperature (T_{dep}) ranging from 720 °C to 820 °C (from top to bottom). The temperature at which the resistivity is minimum is also indicated.

frustration in the film, when the anti-site disorder levels are high [12].

Figure 5 shows the temperature dependent resistivity $\rho(T)$ of the vacuum-cooled SFMO thin films. Over the entire temperature range, $\rho(T)$ of all films are only weakly temperature dependent, and they exhibit a temperature T_{min} at which the resistivity is minimized (ρ_{min}). Below T_{min}, the films behave as weakly insulating and, above it, as weakly metallic; the overall range of $\rho(T)$ is only between 10 and 30% of ρ_{min} over the whole temperature range. $T_{min} = 224, 140, 120$, and 125 K for the films deposited at $T_{dep} = 720, 780, 800$, and 820 °C. The overall resistivity range and ρ_{min} are minimized for the film deposited at the optimal $T_{dep} = 800$ °C. The variation of T_{min} (akin to a weak insulator-to-metal transition temperature) with T_{dep} is qualitatively similar with the variation of the T_C (figure 3); the decrease in ρ_{min} with increased T_{dep} is consistent with the increase of M (figure 4(b)).

Single-crystal SFMO is metallic below the T_C [40], which is 410–450 K [2, 9]. Based on the T_C values shown in figure 3, these films are expected to be metallic below ≈ 295–320 K, consistent with the metallic nature above T_{min}. While the films should be completely metallic, insulating behavior and weak insulator-to-metal transitions have been observed in $\rho(T)$ for SFMO films and ceramics. A similar upturn in the resistivity with a weak metal-to-insulator transition was observed for the well-ordered SFMO ceramics [31] In ceramics, (oxidized) grain boundary effects are often cited as the origin of insulating behavior at low-T, but the $\rho(T)$ is usually orders of magnitude higher than that observed here [42]. Annealing polycrystalline samples at higher temperatures for long times leads to the metal-like electronic transport with low resistivity, presumably because the grain boundaries are reduced [43]. The low-temperature increase in resistivity can be explained by oxygen vacancies, anti-site disorder, anti-site boundary and Fe: Mo non-stoichiometry. The resistivity value of the optimized film in our work is essentially similar to the bulk single crystal value or the best epitaxial films [21, 40, 44]. The variation in T_{min} and ρ_{min} with T_{dep} for our films are similar to effects observed in epitaxial films [21, 44]. Coupling with the variations in crystal quality with T_{dep}, a significant contribution to the variation in $\rho(T)$ for our polycrystalline films should be attributed to local disordered associated with local epitaxial growth, not grain boundaries. A similar conclusion was made for similar observations of SFMO grown on polycrystalline $SrTiO_3$ by Shinde *et al* [21], where the resistivity of their films cooled in vacuum were not controlled by grain boundary effects.

The typical $\rho(T)$ curve for oxygen-cooled SFMO grown on polycrystalline SMWO at 720 °C is shown in figure 6(a). Over the entire range of temperatures, the film exhibits strong semiconducting behavior, with a two orders of magnitude increase in $\rho(T)$. This behavior is in stark contrast to the vacuum-cooled films, even though the Curie temperatures and magnetization are only partially suppressed. Similar $\rho(T)$ curves were observed for oxygen-cooled SFMO films grown at 780 °C and 800 °C on polycrystalline SMWO. The inset of figure 6(a) displays $\rho(T)$ as $\ln\rho$ versus. T^{-1} over the temperature range 230 K to 300 K. This Arrhenius analysis does not support that a thermally activated model describes electron transport, such as that of small polaron hopping [45]. The ln $\rho(T)$ is plotted versus. $T^{-1/4}$ in figure 6(b) for oxygen-cooled SFMO grown on polycrystalline SMWO at different T_{dep}. Linear behavior in such a plot is consistent with a variable range hopping (VRH) model [45, 46], where the jump distance of the localized carrier is variable. The SFMO film grown at 720 °C shows linear dependence of ln $\rho(T)$ with $T^{-1/4}$ in the temperature range of 40–300 K, while the films grown at higher temperatures show linear behavior over almost the entire temperature range. The VRH-type conduction in the double perovskite oxides is explained by the localization of electrons in an impurity band, generated due to the structural distortions, cation disorder or non-stoichiometry [47]. Niebieskikwiat *et al* have shown that the magnetization and structure of SFMO are not influenced by oxygen treatment [17, 31], while resistivity increases on oxygen treatment owing to the formation of $SrMoO_4$ impurities at the grain boundaries. Our observations are similar: the magnetic properties are slightly influenced by the oxygen treatment, whereas the resistivity increased by few orders, likely from oxygenated grain boundaries.

Figure 7(a) shows the resistivity (on a logarithmic scale) measured at 5 K and 300 K for various SFMO thin films plotted as a function of T_{dep} (from the data in figures 5 and 6). The variation of resistivity with T_{dep} is limited to one order of magnitude in all cases. The combination of property variations as T_{dep} is increased for the oxygen-cooled films, including an increased T_C (see figure 3(b)), an increased magnetization (see figure 4(b)) and a negligible quantitative change of the semiconducting resistivity (see figure 7(a)) are consistent with the improved crystallinity of the grain centers with increased T_{dep}, which is the origin of the improved magnetic response with

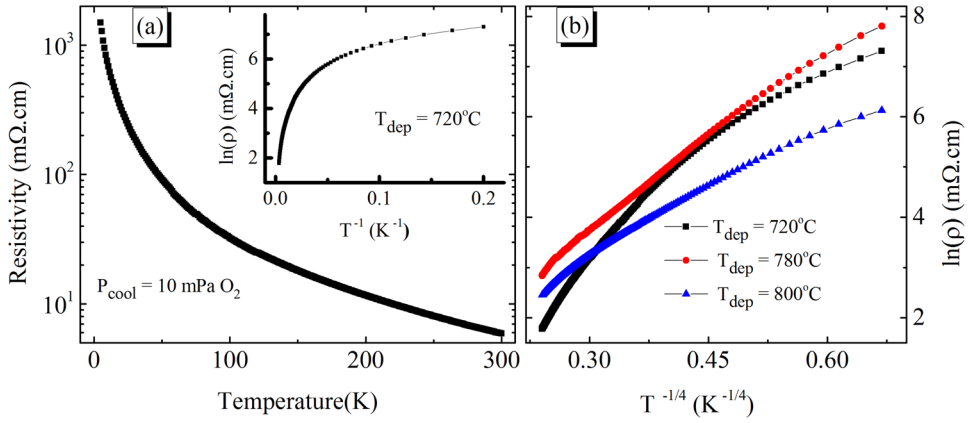

Figure 6. (a) Temperature dependent resistivity of an oxygen-cooled SFMO film grown on polycrystalline SMWO at 720 ° C. The inset shows the log resistivity versus T^{-1} for the same film. (b) The log resistivity versus $T^{-1/4}$ for a series of oxygen-cooled SFMO films grown on polycrystalline SMWO at different temperatures (720, 780, and 800 °C).

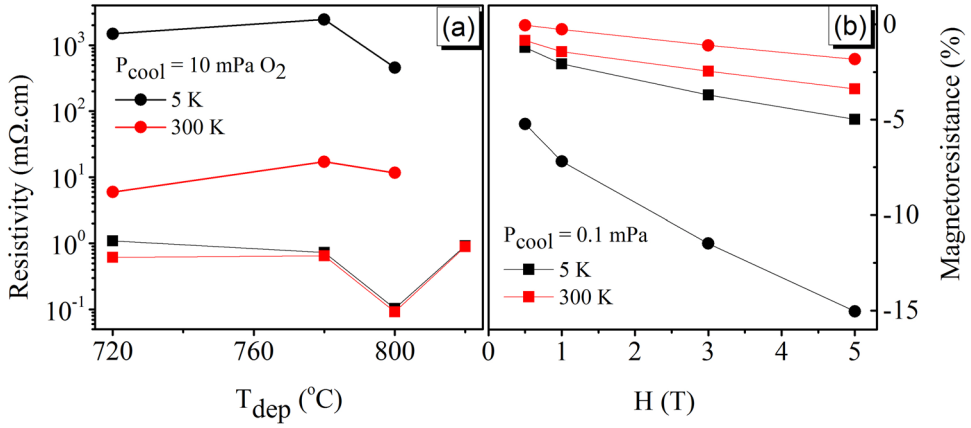

Figure 7. Resistivity of a series of SFMO thin films grown on polycrystalline SMWO plotted as a function of deposition temperature (T_{dep}) for different pressures. (b) Magnetoresistance of SFMO thin films grown on polycrystalline SMWO at 800 °C plotted versus magnetic field. In both plots, measurements were made at 5 K (black) and 300 K (red) for vacuum-cooled (full square) and oxygen-cooled (full circle) films.

increased T_{dep}, while transport is limited by VRH through the oxidized grain boundaries (containing $SrMoO_4$) and the grain cores are likely to retain metallic conductivity reflective of the magnetic properties. For the vacuum-cooled films, the grain boundaries have a similar electronic character to the bulk, and the magnetic properties are still primarily controlled by the crystalline quality of the grain centers. This explanation has been used to describe both bulk ceramics and polycrystalline thin films. Since all these films grew in a grain-over-grain, locally epitaxial fashion (see EBSD maps in figure 2) on a polycrystalline substrate, SMWO, the grain boundaries controlling transport are spatially controlled by the grain boundaries in the substrate. Hence, the transport behavior of these films is similar to the transport of ceramics. A similar set of arguments was used for polycrystalline SFMO films on polycrystalline $SrTiO_3$ substrates [21]. Growth on polycrystalline SMWO substrates offers the possibility of tailoring the mismatch to SFMO to control strains (and defects associated to their relaxation), of providing larger local driving forces to obtain long-range order (and suppress anti-phase disorder) and of grain boundary engineering magnetotransport properties, including the magnetoresistance.

The magnetoresistance (MR) measured at 5 and 300 K for the SFMO films deposited at 800 °C are shown in figure 7(b), plotted versus the magnetic field. The vacuum-cooled and oxygen-cooled SFMO films show a monotonic increase in the negative MR at both temperatures. The 300 K MR of the oxygen- (vacuum-) cooled SFMO film is −1 (−3)% at 5 T. The low value of MR at 300 K of the SFMO film cooled in presence of oxygen is due to the lower T_C of the film (below RT, i.e. 265 K) and thereby the loss of spin polarization. The 5 K MR of the vacuum- (oxygen-) cooled SFMO film is −2 (−15)% at 5 T. The low negative MR observed for vacuum cooled films is due to the grain boundaries having conductivities similar to the bulk of the grain. The oxygen cooled films exhibit a sharp drop in magnetoresistance of −5.2% at a field of 0.5 T. The sharp LFMR in this film is due to the tunneling of charge carriers across the insulating grain boundary barriers at low fields. A LFMR of 5.2% at 0.5 T (15% at 5 T) is significantly larger than polycrystalline films reported in the literature [21, 48], whose grain boundaries arise from growth driven events rather than at predetermined locations in locally epitaxial films on polycrystalline substrates. These results are promising for obtaining property engineered SFMO films

using polycrystalline substrates, but more work is needed to understand how the local structure of grain cores and grain boundaries are influenced by growth parameters, and how they affect the average properties.

4. Conclusion

In conclusion, grazing x-ray diffraction patterns confirm the growth of pure polycrystalline SFMO perovskite on polycrystalline SMWO cooled under as deposited pressure, while those SFMO thin films cooled in the presence of oxygen show a $SrMoO_4$ impurity phase along with the perovskite phase. Thin film deposition was optimized by the average IQ obtained from the Kikuchi pattern indexing. The film deposited at $T_{dep} = 800$ °C and cooled in $P_{cool} = P_{vac}$ shows better crystallinity and the best average IQ value compared to all other thin films. EBSD results for this film show a grain-over-grain epitaxial relationship between grains of substrate and film. The T_C and magnetization at 0.5 T of polycrystalline SFMO thin films grown on SWMO are (i) decreased from values reported for bulk material, (ii) smaller for the films cooled in presence of oxygen, and (iii) increased with the increase of deposition temperature in the range of 720 °C to 800 °C, irrespective of cooling conditions. The reduced magnetization of these thin films can be explained by the presence of anti-site disorder and non-stoichiometry in the local cation content. The temperature-dependent resistivity of polycrystalline SFMO thin films cooled under as deposited pressure show metallic behavior below Tc, but with a weak upturn in resistivity at low temperatures. In contrast, the resistivity of polycrystalline SFMO thin films cooled under oxygen are insulator-like with variable range hopping conduction. The polycrystalline SFMO thin films cooled under oxygen show high LFMR (−5% at 0.5 T) compared to the polycrystalline SFMO thin films cooled under as deposited pressure, which is attributed to the presence of insulating grain boundaries. This work opens the route to tailor the electronic properties by engineering the grain boundaries in thin films.

Acknowledgments

We thank L Gouleuf and J Lecourt for technical support. MS and DP are supported by a PhD fellowship included in the Erasmus Mundus Project IDS-FunMat. M Lacotte received her PhD scholarship from the Ministère de l'Enseignement Supérieur et de la Recherche. Partial support of the French Agence Nationale de la Recherche (ANR), through the program Investissements d'Avenir (ANR-10-LABX-09-01), LabEx EMC3, and the LAFICS are also acknowledged. W.P acknowledged partial support of the Tan Chin Tuan Exchange Fellowship in Engineering. JW thanks support from the Ministry of Education, Singapore under project MOE2013-T2-1-052. PAS and GSR acknowledge the support of the National Science Foundation: grant DMR 1609355.

References

[1] Prellier W *et al* 2000 *J. Phys.: Condens. Matter* **12** 965
[2] Padhan P and Gupta A 2013 *Functional Metal Oxides: New Science and Novel Applications* ed S B Ogale *et al* (New York: Wiley) p 51
[3] Coy L E *et al* 2016 *Appl. Phys. Lett.* **109** 152901
[4] Kayser P *et al* 2017 *Acta. Mater.* **126** 114
[5] Saxena M *et al* 2017 *Scr. Mater.* **130** 205
[6] Azuma M *et al* 2005 *J. Am. Chem. Soc.* **127** 8889
[7] Singh M P *et al* 2007 *Appl. Phys. Lett.* **91** 012503
[8] Huang Y H *et al* 2006 *Science* **312** 254
[9] Kobayashi K I *et al* 1998 *Nature* **395** 677
[10] Saloaro M *et al* 2016 *ACS Appl. Mater. Interfaces* **8** 20440
[11] Sarma D D *et al* 2000 *Solid State Commun.* **114** 465
[12] Garcia-Hernandez M *et al* 2001 *Phys. Rev. Lett.* **86** 2443
[13] Balcells L *et al* 2001 *Appl. Phys. Lett.* **78** 781
[14] Ogale A *et al* 1999 *Appl. Phys. Lett.* **75** 537
[15] Saha-Dasgupta T and Sarma D D 2001 *Phys. Rev.* B **64** 064408
[16] Stoeffler D and Collis S S 2005 *J. Phys.: Condens. Matter* **17** 6415
[17] Niebieskikwiat D *et al* 2001 *Phys. Rev.* B **64** 180406
[18] Chakraverty S *et al* 2011 *Phys. Rev.* B **84** 064436
[19] Fix T *et al* 2005 *J. Appl. Phys.* **98** 023712
[20] Manako T *et al* 1999 *Appl. Phys. Lett.* **74** 2215
[21] Shinde S R *et al* 2003 *J. Appl. Phys.* **93** 1605
[22] Angervo I *et al* 2017 *Appl. Surf. Sci.* **396** 754
[23] Deniz H *et al* 2017 *J. Appl. Phys.* **121** 023906
[24] Kalanda N A *et al* 2016 *J. Electr. Mater.* **45** 3466
[25] Moritomo Y *et al* 2000 *J. Phys. Soc. Japan* **69** 1723
[26] Gateshki M and Igartua J M 2004 *J. Phys.: Condens. Matter* **16** 6639
[27] Eng H W *et al* 2005 *J. Appl. Phys.* **97** 013706
[28] Lacotte M *et al* 2014 *J. Appl. Phys.* **116** 245303
[29] Pravarthana D *et al* 2014 *Appl. Phys. Lett.* **104** 082914
[30] Xia W *et al* 2008 *Physica* B **403** 2189
[31] Niebieskikwiat D *et al* 2004 *Phys. Rev.* B **70** 132412
[32] Kircheisen R and Nonstoichiometry T J 2012 *J. Solid State Chem.* **185** 76
[33] Bessea M *et al* 2002 *J. Cryst. Growth* **241** 448
[34] Goyal A, Paranthaman M P and Schoop U 2004 *MRS Bull.* **29** 552
[35] Zhang Y *et al* 2012 *Acta Mater.* **60** 6486
[36] Kumar N *et al* 2012 *J. Appl. Phys.* **112** 073925
[37] Metasanoja M *et al* 2012 *J. Supercond. Nov. Magn.* **25** 829
[38] Liu G Y *et al* 2003 *J. Phys.: Condens. Matter* **15** 2053
[39] Borges R P *et al* 1999 *J. Phys.: Condens. Matter* **11** L445
[40] Tomioka Y *et al* 2000 *Phys. Rev.* B **61** 422
[41] Venimadhav A *et al* 2004 *Solid State Commun.* **130** 631
[42] Branford W R *et al* 2003 *J. Appl. Phys.* **94** 4714
[43] Huang Y H *et al* 2006 *Phys. Rev.* B **74** 174418
[44] Song J H *et al* 2005 *J. Appl. Phys.* **97** 046105
[45] Poddar A *et al* 2004 *J. Appl. Phys.* **95** 6261
[46] Mott N F 1969 *Phil. Magn.* **19** 835
[47] Popov G *et al* 2003 *Phys. Rev.* B **67** 024406
[48] Kumar N *et al* 2014 *Mater. Lett.* **118** 200